Depot-specific effects of the PPARγ agonist rosiglitazone on adipose tissue glucose uptake and metabolism[S]

William T. Festuccia,[*] Pierre-Gilles Blanchard,[*] Véronique Turcotte,[*] Mathieu Laplante,[†] Meltem Sariahmetoglu,[§] David N. Brindley,[§] and Yves Deshaies[1,*]

Laval Hospital Research Center and Department of Anatomy and Physiology,[*] Faculty of Medicine, Laval University, Quebec, Canada G1V 4G5; Whitehead Institute for Biomedical Research,[†] Massachusetts Institute of Technology, Cambridge, MA 02142; and Signal Transduction Research Group,[§] Department of Biochemistry, University of Alberta, Edmonton, Alberta, Canada T6G 2S2

Abstract **We investigated mechanisms whereby peroxisome proliferator-activated receptor γ (PPARγ) agonism redistributes lipid from visceral (VF) toward subcutaneous fat (SF) by studying the impact of PPARγ activation on VF and SF glucose uptake and metabolism, lipogenesis, and enzymes involved in triacylglycerol (TAG) synthesis. VF (retroperitoneal) and SF (inguinal) of rats treated or not for 7 days with rosiglitazone (15 mg/kg/day) were evaluated in vivo for glucose uptake and lipogenesis and in vitro for glucose metabolism, gene expression, and activities of glycerolphosphate acyltransferase (GPAT), phosphatidate phosphatase-1 (or lipin-1), and diacylglycerol acyltransferase. Rosiglitazone increased SF glucose uptake, GLUT4 mRNA, and insulin-stimulated glucose oxidation, conversion to lactate, glycogen, and the glycerol and fatty acid components of TAG. In VF, only glucose incorporation into TAG-glycerol was stimulated by rosiglitazone and less so than in SF (1.5- vs. 3-fold). mRNA levels of proteins involved in glycolysis, Krebs cycle, glycogen synthesis, and lipogenesis were markedly upregulated by rosiglitazone in SF and again less so in VF. Rosiglitazone activated TAG-glycerol synthesis in vivo (2.8- vs. 1.9-fold) and lipin activity (4.6- vs. 1.5-fold) more strongly in SF than VF, whereas GPAT activity was increased similarly in both depots. The preferential increase in glucose uptake and intracellular metabolism in SF contributes to the PPARγ-mediated redistribution of TAG from VF to SF, which in turn favors global insulin sensitization.—** Festuccia, W. T., P-G. Blanchard, V. Turcotte, M. Laplante, M. Sariahmetoglu, D. N. Brindley, and Y. Deshaies. **Depot-specific effects of the PPARγ agonist rosiglitazone on adipose tissue glucose uptake and metabolism. *J. Lipid Res.* 2009.** 50: **1185–1194.**

Supplementary key words glucose oxidation • lipogenesis • glycerol 3-phosphate acyltransferase • lipin • diacylglycerol acyltransferase • visceral fat • subcutaneous fat

White adipose tissue (WAT) plays an important role in whole-body homeostasis by acting both as an energy reservoir and as an endocrine gland secreting several adipokines that impact major metabolic tissues, such as the liver, muscle, and brain. The importance of WAT in the maintenance of a healthy whole-body homeostasis is highlighted by the direct relationship of disturbances in WAT function (obesity and lipodystrophy) with the development of several morbidities, such as Type 2 diabetes, cancer, and atherosclerosis.

Peroxisome proliferator-activated receptorγ (PPARγ), a nuclear receptor mainly expressed in WAT, plays a key role in regulating adipose metabolic and endocrine functions. PPARγ is a master regulator of adipocyte differentiation, and its activation in vivo results in adipose tissue remodeling associated with lipid redistribution from visceral fat (VF) to subcutaneous fat (SF) (1–3). More specifically, PPARγ activation in both humans and rodents is associated with an enhanced ability of SF to take up and store fatty acids, especially those derived from lipoprotein-bound triacylglycerol (TAG) through lipoprotein lipase (4). Directing fat away from VF to SF depots may constitute one mechanism whereby PPARγ agonism prevents the deleterious effects of VF accumulation on the development of the metabolic syndrome and the progression to cardiovascular disease.

Glucose is the major substrate metabolized in WAT. It is used not only for the synthesis of glycerol 3-phosphate, the carbon backbone of TAG, and fatty acids by de novo lipogenesis, but it is also used to generate energy that supports

This work was supported by a grant from the Canadian Institutes of Health Research to Y.D. and from the Heart and Stroke Foundation of Canada to D.N.B. P-G.B. was the recipient of a Frederick Banting and Charles Best Canada Graduate Scholarships, Doctoral Award from the Canadian Institutes of Health Research.

Manuscript received 2 December 2008 and in revised form 29 January 2009.

Published, JLR Papers in Press, February 5, 2009.
DOI 10.1194/jlr.M800620-JLR200

Abbreviations: CIDEC, cell death-inducing DNA fragmentation factor-α-like effector; DGAT, diacylglycerol acyltransferase; G6PDH, glucose 6-phosphate dehydrogenase; GLUT, glucose transporter; GPAT, glycerol 3-phosphate acyltransferase; GyS2, glycogen synthase 2; ME, malic enzyme; NEFA, nonesterified fatty acid; PAP-1, phosphatidate phosphatase-1; PEPCK, phosphoenolpyruvate carboxykinase; PPARγ, peroxisome proliferator-activated receptor γ; SF, subcutaneous fat; SREBP1, sterol regulatory binding protein 1; TAG, triacylglycerol; UDPG-PPL, UDP-glucose pyrophosphorylase; VF, visceral fat; WAT, white adipose tissue.

[1]To whom correspondence should be addressed.
e-mail: yves.deshaies@phs.ulaval.ca

[S]The online version of this article (available at http://www.jlr.org) contains supplementary data in the form of one figure and one table.

fatty acid esterification and TAG synthesis and other adipocyte functions. Most of the glucose (~50%) taken up by the adipocytes is normally used to synthesize the glycerol and fatty acid components of TAG, with the remainder being directed toward oxidation (~30%) and the synthesis of lactate and glycogen (5). Although PPARγ ligands, due to their positive effects on whole body glucose homeostasis, are widely used in the treatment of insulin resistance, little is known about their effects on WAT glucose metabolism. Deletion of one PPARγ allele is associated with an impairment of WAT expression of several genes implicated in glucose uptake, glycolysis, glycogen synthesis, and the pentose pathway, suggesting a key involvement of PPARγ in controlling WAT glucose metabolism (6). Whether the above changes in WAT gene expression translate into alterations of the corresponding metabolic processes in vivo and whether such changes are depot specific, as is the case for fat accretion, remains to be investigated.

WAT provides an important contribution to whole-body glucose homeostasis (5), and changes in adipocyte intracellular glucose metabolism could be part of the fat redistribution induced by PPARγ agonism. This study assesses the effects of PPARγ activation in vivo on glucose metabolism in retroperitoneal and inguinal depots, which are representative of VF and SF, respectively. Rats treated with the thiazolidinedione, rosiglitazone, were evaluated in vivo for glucose uptake and lipogenesis, in vitro for glucose oxidation, and for its conversion to lactate, TAG, and glycogen. We also assessed the activities of key enzymes of TAG synthesis along with an extensive comparative analysis of the gene expression profile of VF and SF to investigate the mechanisms of rosiglitazone action.

RESEARCH DESIGN AND METHODS

Animals and treatment

Experimental procedures were performed in accordance with the Canadian Guide for the Care and Use of Laboratory Animals and received prior approval of the Laval University animal care committee. Male Sprague-Dawley rats (Charles River, St. Constant, QC, Canada) were matched by weight and divided into control and rosiglitazone-treated groups that received a powdered rodent diet (Charles River #5075, Woodstock, ON, Canada; energy density 12.9 kJ/g, 62.5% carbohydrate, 4.5% fat, and 18% protein) alone (control) or supplemented with the PPARγ agonist rosiglitazone (Avandia) at a dose of 15 mg/kg·day for 7 days. Rats were kept at 23 ± 1°C with a 12 h light/dark cycle. A high-carbohydrate diet was selected to maximize glucose flux. PPARγ-induced adipose remodeling, insulin sensitization, and lipemia improvement occur independently of dietary composition (4, 7). The dose of rosiglitazone was chosen based on preliminary studies that showed its effectiveness to redistribute fat from visceral to subcutaneous depots within a 3 week period of treatment. One week of treatment was chosen to investigate the initial effects of rosiglitazone involved in this lipid redistribution. Ground rosiglitazone was mixed with the powdered chow diet, and the desired dose (15 mg/kg·day) was achieved by adjusting the amount of drug to the average food consumption and body weight of rats every other day.

Glucose uptake in vivo

The rate of glucose uptake by adipose depots was estimated in vivo essentially as previously described (8, 9). Briefly, 0.2 ml of a 2-deoxy-1-^{3}H-glucose (30 μCi, 11 Ci/mmol; New England Nuclear) and 0.9% NaCl solution were injected through a catheter inserted in the jugular vein, and 0.2 ml of blood was collected at 1, 3, 5, 10, 20, 40, and 60 min after label injection for radioactivity and glucose estimation. Jugular catheters were inserted 3 days before the glucose uptake assay. After 60 min, rats were killed by overdose of ketamine/xylazine, and tissues were used for determining the content of 2-deoxy-[1-^{3}H]glucose 6-phosphate. Rates of glucose uptake were calculated as previously described (9). Blood glucose levels did not significantly change during the sampling period in either group, a requirement of the technique used.

Tissue glycogen content

Measurement of WAT glycogen content was performed as described previously (10).

Lipogenesis in vivo

Fed, nonanesthetized rats were injected with 185 GBq/ml $^{3}H_2O$ (Amersham; 3 mCi in 0.5 ml sterile saline solution, intraperitoneal injection). One hour after injection, rats were killed by decapitation, blood samples were collected, and the specific radioactivity of plasma water was determined. Liver, VF (retroperitoneal), and SF (inguinal) were removed and processed for measurement of label incorporation into TAG. Tissue total lipids were extracted with 2:1 chloroform:methanol as described previously (11) and processed for the measurement of ^{3}H incorporation into fatty acid component of TAG (12). Incorporation of ^{3}H into TAG-glycerol was estimated by the difference between incorporation into total lipids and fatty acids. Rates of tissue fatty acid and glycerol synthesis were calculated assuming that each glycerol and each fatty acid incorporated into TAG contained 3.3 and 13.3 atoms of tritium, respectively (13, 14).

Glucose uptake and conversion to its metabolites in vitro

Glucose conversion to its metabolites in vitro was measured as described previously (15). Fat explants were used rather than isolated adipocytes to avoid metabolic stress associated with collagenase digestion and to preserve the in vivo microenvironment as much as possible. Interpretation of the data should therefore take into account the possibility that cell populations other than mature adipocytes may have contributed to treatment effects. Briefly, fat explants (20–25 mg) of SF and VF were incubated in 1 ml of Krebs-Ringer bicarbonate buffer (in mmol/l): 118 NaCl, 4.8 KCl, 1.25 $CaCl_2$, 1.2 KH_2PO_4, 1.2 $MgSO_4$, 25 $NaHCO_3$, and 5.5 [U-^{14}C]glucose (0.5 μCi/tube, 3 mCi/mmol; Amersham) supplemented with 2.5% fatty acid-free BSA (Sigma-Aldrich, Oakville, ON, Canada), pH 7.4. Vials were closed with a rubber stopper, gassed with 5% CO_2 and 95% O_2, and incubated at 37°C for 1 h in the presence or absence of insulin (100 pmol/l). The insulin concentration was chosen to approximate to that found in vivo in the fasting state. At the end of the incubation, reactions were stopped with H_2SO_4, and benzathonium hydroxide was injected with a syringe and needle into a strip of paper previously positioned in the rubber stopper to trap CO_2. Explants were removed and destined to either lipid or glycogen extraction as described above, and media were frozen for later lactate assay (BioVision Research Products, CA). A similar procedure was used for glucose uptake estimation, the exception being the replacement of glucose by 2-deoxy-[1-^{3}H]glucose (0.5 μCi/tube). Explants were processed for determination of content of 2-deoxy-[1-^{3}H]glucose 6-phosphate as described previously (9). Results are expressed as μmol/μg DNA/h to correct for cell number. The DNA content was determined using the DNeasy Tissue Kit (Qiagen, Mississauga, ON, Canada) following the manufacturer's instructions.

TABLE 1. Energy balance determinants and serum hormones and metabolites in rosiglitazone-treated rats

	Control	RSG
Initial body weight (g)	256 ± 2	256 ± 2
Final body weight (g)	308 ± 3	321 ± 4*
Body weight gain (g)	52 ± 3	63 ± 3*
Food intake (g)	197 ± 4	206 ± 4
Food efficiency (%)[a]	25.2 ± 0.9	29.8 ± 1.2*
VF (g)	1.18 ± 0.06	1.13 ± 0.12
SF (g)	1.70 ± 0.07	2.04 ± 0.09*
Insulin (pmol/l)	235 ± 21	114 ± 10*
Adiponectin (μg/ml)	3.3 ± 0.5	17.1 ± 0.7*
Glucose (mmol/l)	10.0 ± 1.5	12.2 ± 1.2
NEFA (mmol/l)	0.099 ± 0.009	0.054 ± 0.01*
TAG (mmol/l)	2.36 ± 0.24	0.96 ± 0.14*

Data are means ± SEM of six rats. * $P < 0.05$. RSG, rosiglitazone.
[a] Calculated as g body weight gain/100 g food ingested.

Enzymatic activities

Phosphoenolpyruvate carboxykinase (PEPCK) activity was assayed in 100,000 *g* supernatants obtained after homogenization of adipose tissue in a buffer (pH 7.5) containing 20 mmol/l triethanolamine, 0.25 mol/l sucrose, 5 mmol/l mercaptoethanol, and 1 mmol/l EDTA. PEPCK activity was determined by the method of Chang and Lane (16), based on the incorporation of $H_2{}^{14}CO_3$ (0.074 MBq) into acid-stable product as described previously (17). Total protein concentration in the homogenate was determined by the bicinchoninic acid method (18). LPL activity was measured by incubating 100 μl of adipose tissue homogenates for 1 h at 28°C with 100 μl of a substrate mixture consisting of 0.2 mol/l Tris-HCl buffer, pH 8.6, which contained 10 MBq/l [*carboxyl*-^{14}C]triolein (Amersham, Oakville, ON, Canada) and 2.52 mmol/l cold triolein emulsified in 50 g/l gum arabic, as well as 20 g/l fatty acid-free BSA, 10% porcine serum as a source of apolipoprotein C-II, and either 0.2 or 2 M NaCl. Free oleate released by LPL was then separated from intact triolein, and sample ^{14}C radioactivity was determined in a scintillation counter. LPL activity was calculated by subtracting lipolytic activity determined in a final NaCl concentration of 1 M (non-LPL activity) from total lipolytic activity measured in a final NaCl concentration of 0.1 M. LPL activity was expressed as microunits [1 μU = 1 μmol nonesterified fatty acid (NEFA) released per hour of incubation at 28°C]. The activity of LPL is expressed per total adipose depot to reflect the relative contribution of specific depots to TAG kinetics. Glycerol 3-phosphate acyltransferase (GPAT) activity was measured as described previously (19, 20) with some modifications. Adipose tissues were homogenized in buffer A (10 mM Tris-HCl, 250 mM sucrose, 1 mM EDTA, and 1 mM DTT, pH 7.5) and centrifuged at 600 *g*, 4°C for 10 min. The supernatant was removed and centrifuged at 100,000 *g* for 1 h at 4°C. Pellets were resuspended in buffer A and evaluated for GPAT activity after a 15 min incubation on ice with or without 2 mM (final concentration) *N*-ethylmaleimide. The assay mixture was composed of 75 mM Tris-HCl, pH 7.5, 4 mM $MgCl_2$, 1 mg/ml BSA (essentially fatty acid free), 8 mM NaF, 100 μM palmitoyl-CoA, and 500 μM of ^{14}C-glycerol 3-P (0.5 μCi/tube, 100 mCi/mmol; Amersham). Reactions were stopped with 3 ml of chloroform:methanol (1:2, v/v) and 0.6 ml of 1% perchloric acid. After 5 min, 1 ml of chloroform and 1 ml of 1% perchloric acid were added, tubes were shaken vigorously, and the upper methanolic phase was discarded. The lower phase was washed three times with 1% perchloric acid, evaporated, and counted. Diacylglycerol acyltransferase (DGAT) activity was measured as described previously (21) with some modifications. Adipose tissues were homogenized in buffer A and centrifuged twice at 12,000 *g*, 4°C for 10 min. The supernatant was removed and centrifuged at 100,000 *g* for 1 h at 4°C. Pellets were resuspended in buffer A and evaluated for DGAT activity. The assay mixture was composed of 150 mM Tris-HCl, pH 7.5, 8 mM $MgCl_2$, 1 mg/ml BSA, 100 μM 1-[^{14}C]palmitoyl-CoA (0.25 μCi/tube, 50 mCi/mmol; Amersham), and 0.8 mM of 1,2-diacylglycerol in absolute ethanol. Reactions were stopped with 1.5 ml of propanol-2:heptane:water (80:20:2, v/v/v). After 5 min, 1 ml of heptane and 0.5 ml of water were added and tubes were shaken vigorously. The heptane layer was removed and washed twice with 0.5 N NaOH:ethanol:water (10:50:50, v/v/v), evaporated, and counted. It has been demonstrated that >90% of labeled material present at the final heptane phase migrated like TAG upon thin layer chromatography in petroleum ether/diethyl ether/acetic acid (80/20/1, v/v/v) solvent (21).

Phosphatidate phosphatase-1 activity and lipin-1 concentration

Adipose tissues were homogenized in 0.25 M sucrose containing 2 mM DTT [to stabilize phosphatidate phosphatase-1 (PAP1)

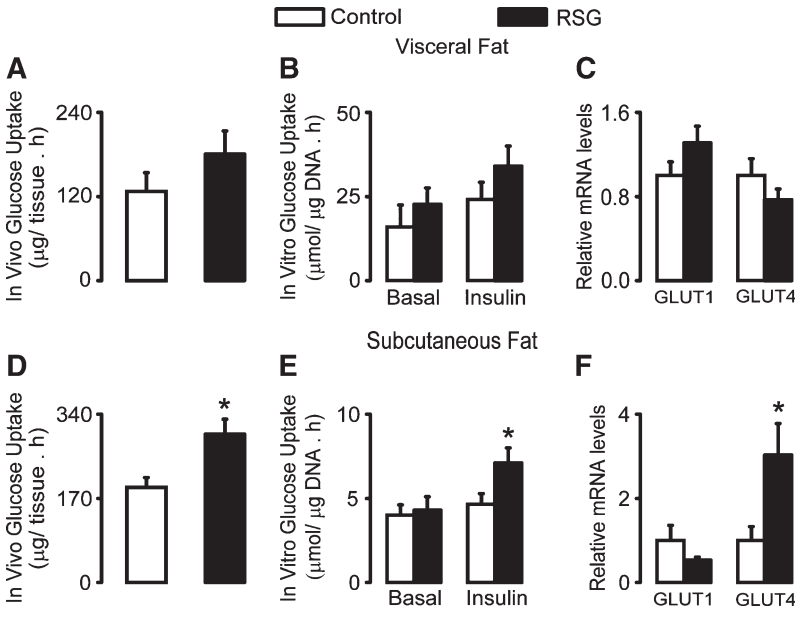

Fig. 1. In vivo (A, D) and in vitro (B, E) rates of glucose uptake and mRNA levels of GLUT1 and GLUT4 (C, F) in visceral fat (upper panels) and subcutaneous fat (lower panels) of rats treated or not with rosiglitazone (RSG) for 7 days. Each column represents the mean ± SEM of 6–12 rats. * $P < 0.05$ versus untreated control.

activity] and Protease Inhibitor cocktail (EDTA-free; Roche Diagnostics, Indianopolis, IN). The homogenates were then centrifuged at 4000 r.p.m. for 10 min at 4°C and infranatants were collected. For the PAP1 assay, Tween 20 (0.15%) was added to the homogenates to stabilize and increase the PAP1 activity. The assays were performed essentially as described previously (22, 23). The incubations were contained in a final volume of 100 μl:100 mM Tris/maleate buffer, pH 6.5, 5 mM $MgCl_2$, 2 mg/ml BSA (essentially fatty acid free), and 0.6 mM phosphatidic acid labeled with [^{3}H]palmitate (1×10^5 dpm/assay) that was dispersed in 0.4 mM phosphatidylcholine, 1 mM EDTA, and 1 mM EGTA. Reactions were stopped after incubation at 37°C for 60 min with 2.2 ml of chloroform containing 0.08% olive oil as carrier, and DAG was purified using basic alumina (22, 23). Total PAP activities were calculated from measurements at three different protein concentrations to ensure the proportionality of the assay. Parallel incubations were performed in the presence of excess (5 mM) N-ethylmaleimide (NEM) to inhibit PAP1 and to compensate for any PAP2 activity in this assay.

Western blot analysis of lipin-1

Identical amounts of protein were electrophoresed in 8% SDS-polyacrylamide gels and transferred onto nitrocellulose membranes (Bio-Rad). Membranes were blocked with Odyssey blocking buffer (Li-Cor Biosciences, Lincoln, NE) and then incubated with rabbit lipin-1 antibody followed by IRDye 800 goat anti-rabbit IgG (20). Images obtained at 800 nm were quantified using the Odyssey: Imager System (Li-Cor).

RNA isolation and analysis

VF and SF total RNA isolation, reverse transcription, and quantification by real-time PCR were performed as described previously (24). Primers used for the PCR reactions are described in Supplementary Table I. Results are expressed as the ratio between the expression of the target gene and the housekeeping gene 36B4, the expression of which is not significantly affected by rosiglitazone treatment.

Serum determinations

Serum glucose concentrations were measured with the YSI 2300 STAT Plus glucose analyzer (YSI, Yellow Springs, OH). Plasma adiponectin and insulin levels were determined by RIA (Linco Research, St. Charles, MO) with rat insulin as standard. Serum TAG and NEFA levels were measured by enzymatic methods (Roche Diagnostics, Montreal, QC, Canada, and Wako Chemicals, Richmond, VA, respectively).

Statistical analysis

Results are expressed as means ± SEM. Simple effects of rosiglitazone treatment were analyzed by Student's unpaired *t*-test. $P < 0.05$ was taken as the threshold of significance.

RESULTS

Final body weight and body weight gain were significantly increased (5 and 22%, respectively) after 7 days of rosiglitazone treatment (**Table 1**). The higher body weight of rosiglitazone-treated rats was associated with an increase in food efficiency (18%) and SF mass (20%), whereas food intake and VF mass were not significantly different. Rosiglitazone significantly increased plasma levels of adiponectin (400%), reduced those of insulin (−50%), NEFA (−45%), and TAG (−60%), but did not alter serum glucose levels. Rosiglitazone, therefore, exerted its expected metabolic actions.

Glucose uptake in VF and mRNA levels of GLUT1 and 4 were not significantly affected by rosiglitazone (**Fig. 1A–C**). In contrast, in SF, rosiglitazone increased glucose uptake measured both in vivo and in vitro in the presence of low insulin levels (36 and 52%, respectively; Fig. 1D, E), an effect that was associated with a 2-fold increase in SF GLUT4, but not GLUT1 mRNA levels (Fig. 1F).

As in the case of in vitro glucose uptake, chronic treatment with rosiglitazone did not affect VF or SF intracellular glucose metabolism in vitro under basal (without insulin) conditions (see supplementary Fig. IA for representative examples). As expected, in adipose explants from control rats,

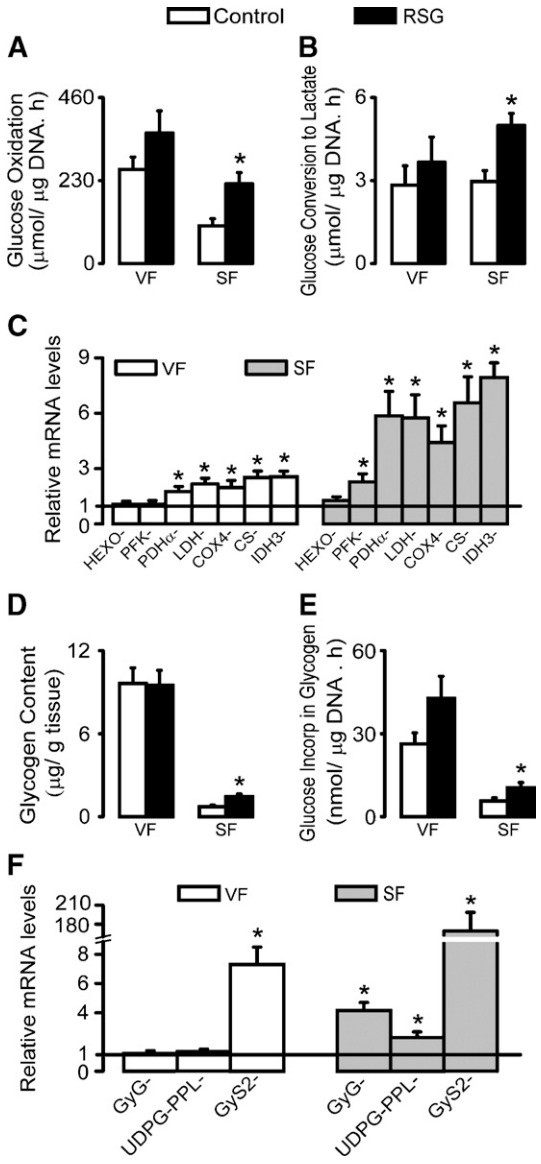

Fig. 2. In vitro insulin-stimulated rates of glucose oxidation (A), conversion to lactate (B), tissue glycogen content (D), its synthesis from glucose (E), and mRNA levels of proteins involved in glycolysis (C) and glycogen synthesis (F) in VF and SF of rats treated or not with rosiglitazone (RSG) for 7 days. Each column represents the mean ± SEM of 12 rats. * $P < 0.05$ versus untreated control.

addition of low (1 pM) insulin did not stimulate any of the determinants of intracellular glucose metabolism investigated (see supplementary Fig. IB for representative examples). The following results therefore focus on the depot specificity of action of chronic rosiglitazone on glucose metabolism evaluated in the presence of low insulin (approximating fasting levels in vivo). Similar to uptake, insulin-stimulated glucose oxidation (**Fig. 2A**) and conversion to lactate (Fig. 2B) were not affected by rosiglitazone in VF. This was despite a significant increase (~2-fold) in tissue mRNA levels of pyruvate dehydrogenase subunit α and lactate dehydrogenase and of the mitochondrial cytochrome oxidase 4, citrate synthase, and isocitrate dehydrogenase 3 (Fig. 2C), which are involved in respiratory chain and Krebs cycle, respectively. No effect of rosiglitazone was seen in VF glycogen content (Fig. 2D), its synthesis from glucose (Fig. 2E), and mRNA levels of glycogenin and UDP-glucose pyrophosphorylase (UDPG-PPL) proteins, which acts as a primer and generates UDP-linked glucose for glycogen synthesis, respectively, despite a 7-fold increase in glycogen synthase 2 (GyS2) mRNA (Fig. 2F). In SF, however, rosiglitazone significantly increased rates of insulin-stimulated glucose oxidation (112%; Fig. 2A), conversion to lactate (60%; Fig. 2B), and mRNA levels of phosphofructokinase A (~3-fold), pyruvate dehydrogenase subunit α (~6-fold), lactate dehydrogenase (~6-fold), cytochrome oxidase 4 (~4-fold), citrate synthase (~7-fold), and isocitrate dehydrogenase 3 (~8-fold) (Fig. 2C). In SF, rosiglitazone also enhanced insulin-stimulated incorporation of glucose into glycogen (85%; Fig. 2E), which was associated with a marked increase in tissue glycogen content (102%; Fig. 2D) and mRNA levels of glycogenin (~4-fold), UDPG-PPL (~2-fold), and GyS2 (~160-fold) (Fig. 2F).

Having shown major depot-specific differences in glucose handling in response to rosiglitazone, we investigated whether such specificity extended to lipid metabolism. Rosiglitazone significantly increased insulin-stimulated glucose incorporation into VF TAG through enhanced synthesis of the glycerol moiety of TAG from glucose (**Fig. 3A**). This was associated with a significant increase in VF mRNA levels (Fig. 3B) of major enzymes involved in NADPH generation, synthesis of glycerol 3-phosphate, fatty acids, and TAG, including glucose 6-phosphate dehydrogenase (G6PDH; 3.3-fold), malic enzyme (ME; 3.3-fold), sterol regulatory binding protein 1 (SREBP1; 1.5-fold), glycerol 3-phosphate dehydrogenase 1 (1.7-fold), and cell death-inducing DNA fragmentation factor-α-like effector (CIDEC, also known as fat-specific protein 27; 3.2-fold). Rosiglitazone significantly increased insulin-stimulated glucose incorporation into TAG also in SF; however, in contrast with VF, this resulted from increased synthesis of both the glycerol and fatty acid fractions of TAG from glucose (2.5- and 6.3-fold, respectively; Fig. 3C). Rosiglitazone increased mRNA levels of G6PDH, ME, FAS, SREBP1, glycerol 3-phosphate dehydrogenase 1, and CIDEC (Fig. 3D) to a greater extent in SF compared with VF.

Because rosiglitazone positively affected glucose incorporation into TAG in vitro, we investigated adipose tissue lipogenesis in vivo by the incorporation of ^{3}H from $^{3}H_2O$ into both the glycerol and fatty acid components of TAG. This technique allows the estimation not only of fatty acid synthesis from all carbon sources, including those from glucose, but also glycerol synthesis from glucose by partial glycolysis (up to the level of triose phosphates) and glyceroneogenesis, although not that from glycerokinase. Rosiglitazone markedly increased the synthesis of the glycerol component of TAG in SF in vivo but less so in VF (2.8- and 1.9-fold, respectively; **Fig. 4**). In contrast, the agonist did not affect rates of de novo fatty acid synthesis in any of the depots. Liver synthesis of the fatty acid and glycerol components of TAG was not affected by rosiglitazone. Consistent with TAG-glycerol synthesis, rosiglitazone markedly increased PEPCK activity in both SF (5.7-fold) and VF (2.3-fold). Lipoprotein lipase activity, which provides fatty acids from plasma lipoprotein-TAG, was also significantly stimulated by rosiglitazone in SF (7.4-fold) but much less so in VF (1.3-fold).

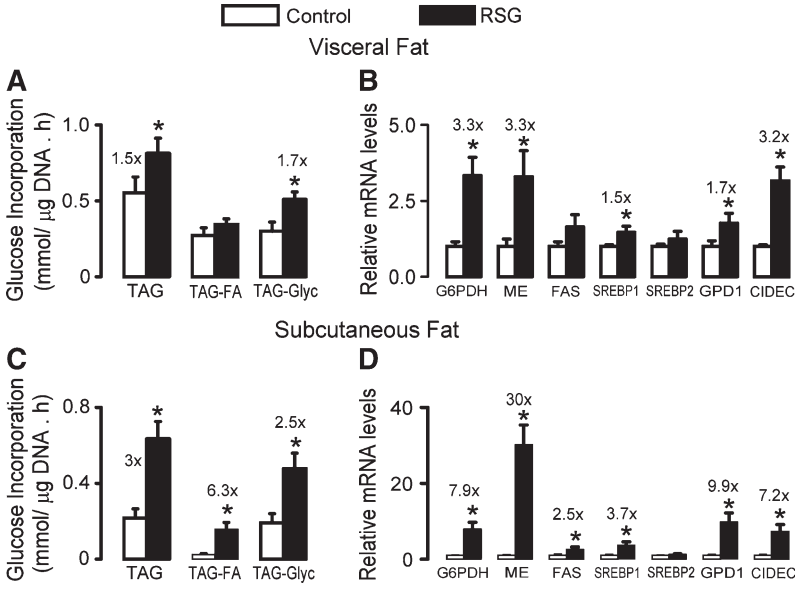

Fig. 3. In vitro insulin-stimulated rates of glucose incorporation into TAG and its fatty acid and glycerol components and mRNA levels of proteins involved in these processes in VF (A, B) and SF (C, D) of rats treated or not with rosiglitazone (RSG) for 7 days. Each column represents the mean ± SEM of 12 rats. * $P < 0.05$ versus untreated control.

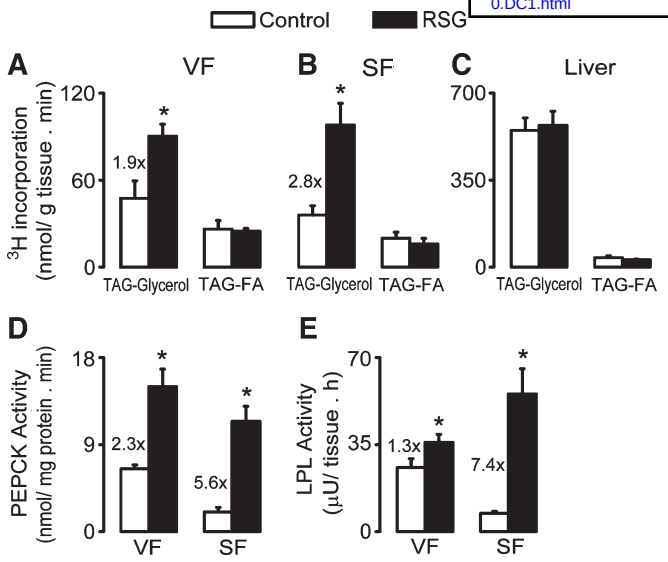

Fig. 4. In vivo incorporation of ^3H from ^3H_2O into the glycerol and fatty acid components of TAG in VF (A), SF (B), and liver (C) and activities of PEPCK (D) and LPL (E) in VF and SF of rats treated or not with rosiglitazone (RSG) for 7 days. Each column represents the mean ± SEM of six rats. * $P < 0.05$ versus untreated control.

To further elucidate the depot-specific mechanisms by which rosiglitazone impacts TAG synthesis in adipose tissue in vivo, the activities of key enzymes involved in this process (summarized in **Fig. 8**) were investigated, including GPAT (**Fig. 5**), PAP1/lipin (**Fig. 6**), and DGAT (**Fig. 7**). Rosiglitazone increased total GPAT activity equally in VF and SF as a result of an increase in both NEM-resistant and sensitive activities (Fig. 5A, C). This was associated with a significant increase in VF and SF mRNA levels of GPAT isoforms 1 and 3, but not 4 (Fig. 5B, D). Rosiglitazone significantly increased SF and VF PAP-1 activity (Fig. 6A, E), and these changes were paralleled by increases in lipin 1 protein concentrations (Fig. 6D, H). The increases in PAP1 activity (4.6- vs. 1.5-fold, respectively; Fig. 6A, E), and to a lesser extent lipin 1 protein (Fig. 6D, H), were greater in SF compared with VF, and these differences were associated with a more marked increase in mRNA levels of lipin 1 and lipin 1B in SF compared with VF (~8- vs. 3.6-fold, respectively; Fig. 6B, C, F, G). Finally, rosiglitazone treatment was associated with a significant increase in VF and SF DGAT activity and mRNA levels of its isoform DGAT1 (Fig. 7A, B, D, E). In SF, however, rosiglitazone additionally increased DGAT2 mRNA levels (Fig. 7F).

DISCUSSION

To further elucidate the mechanisms involved in fat redistribution and insulin sensitization induced by PPARγ activation in vivo, this study investigated the impact and mechanisms of action of rosiglitazone on VF and SF glucose metabolism and lipogenesis. In SF, rosiglitazone markedly increased glucose uptake and insulin-stimulated glucose oxidation, conversion to lactate, and incorporation into glycogen and into both the glycerol and fatty acid components of TAG. The in vitro effects occurred only in the presence of insulin at a dose (equivalent to in vivo fasting levels) that was too low to affect glucose metabolism in controls, which demonstrates that rosiglitazone increases the responsiveness of SF glucose metabolism to the action of insulin. In VF, only glucose incorporation into the glycerol component of TAG was significantly stimulated by rosiglitazone, and it was so to a lesser extent than in SF. The mRNA levels of proteins involved in glycolysis, Krebs cycle, glycogen synthesis, and lipogenesis were markedly upregulated by rosiglitazone in SF, but less so in VF. Rosiglitazone also induced a much more marked increase in the in vivo synthesis of the glycerol component of TAG, and LPL and lipin activities in SF compared with VF, whereas GPAT activity was similarly increased in both depots. A depot-specific increase in SF DGAT2 mRNA levels was also induced by rosiglitazone, although enzyme activity was elevated to similar levels in both SF and VF. Collectively, these results point toward an involvement of SF glucose metabolism in the fat redistribution and improved glucose disposal induced by PPARγ agonism in vivo.

This study confirmed that the well-established positive actions of rosiglitazone on insulin sensitivity and lipemia occur despite increased body weight gain and subcuta-

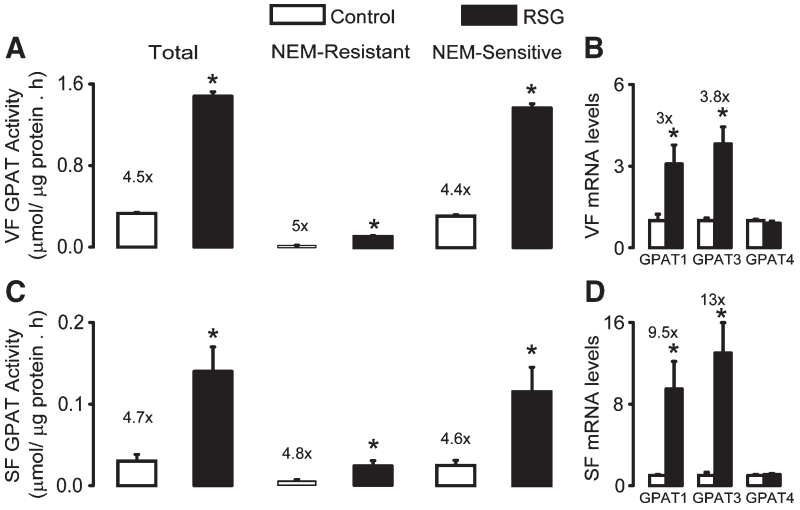

Fig. 5. Total, NEM-resistant, and NEM-sensitive GPAT activities and mRNA of the GPAT isoforms 1, 3, and 4 in VF (A, B) and SF (C, D) of rats treated or not with rosiglitazone (RSG) for 7 days. Each column represents the mean ± SEM of six rats. * $P < 0.05$ versus untreated control.

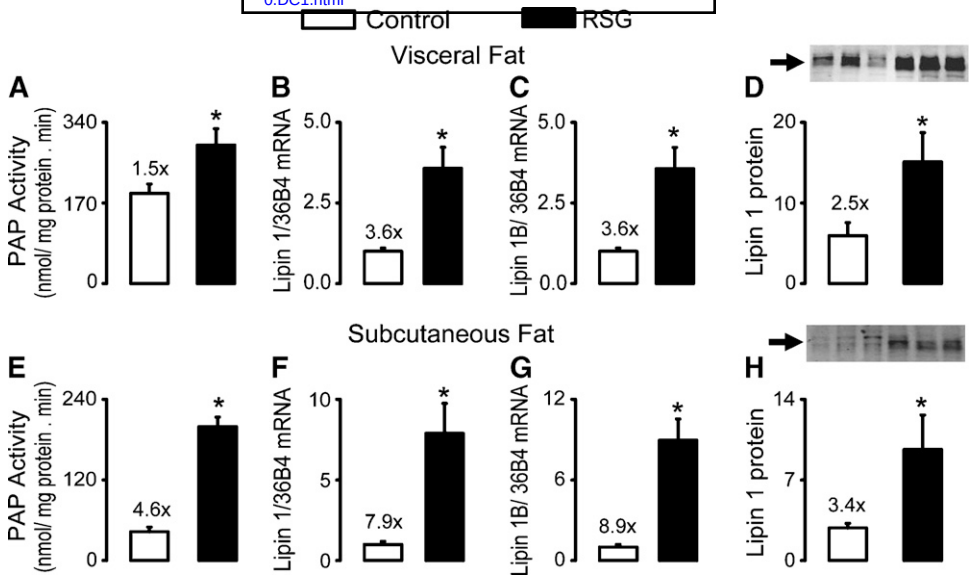

Fig. 6. PAP1 activity, mRNA levels of the lipin isoforms 1 and 1B, and protein content in VF (A–D) and SF (E–H) of rats treated or not with rosiglitazone (RSG) for 7 days. Each column represents the mean ± SEM of six rats. * $P < 0.05$ versus untreated control. Representative Western blots are shown for three untreated (left) and three rosiglitazone-treated rats (right).

neous adiposity. In the present conditions, rosiglitazone only tended to reduce VF mass; however, longer exposure to higher doses clearly reduce VF accretion in the rat (4, 7). Fat redistribution from VF to SF, a hallmark of PPARγ agonism, is thought to play a role in the insulin-sensitizing action of PPARγ agonists in humans (1). We previously demonstrated that enhanced lipid flux to SF, but not VF, especially from fatty acids originating from the hydrolysis of lipoprotein-bound TAG by lipoprotein lipase, constitutes an important component of fat redistribution induced by PPARγ agonism, as confirmed here (4, 7). Here, we extend our mechanistic understanding of such fat redistribution by showing that the increased flux of lipids to SF occurs in conjunction with a marked depot-specific upregulation of glucose uptake and intracellular metabolism. Rosiglitazone increased SF glucose uptake in vivo and in vitro in the presence of low insulin levels, likely in part as a result of the elevated content of the insulin-responsive GLUT4. Furthermore, corroborating a previous study showing that deletion of one PPARγ allele markedly reduces WAT energy production and ATP content (6), rosiglitazone-induced PPARγ activation robustly increased aerobic (glucose oxidation) and anaerobic (glucose conversion to lactate) glycolysis and thus energy production in SF. This is consistent with the concomitant enhancement of glucose uptake, elevated mRNA levels of enzymes of glycolysis, Krebs cycle, and mitochondriogenesis. Although some of the above-mentioned genes were also upregulated in VF, the magni-

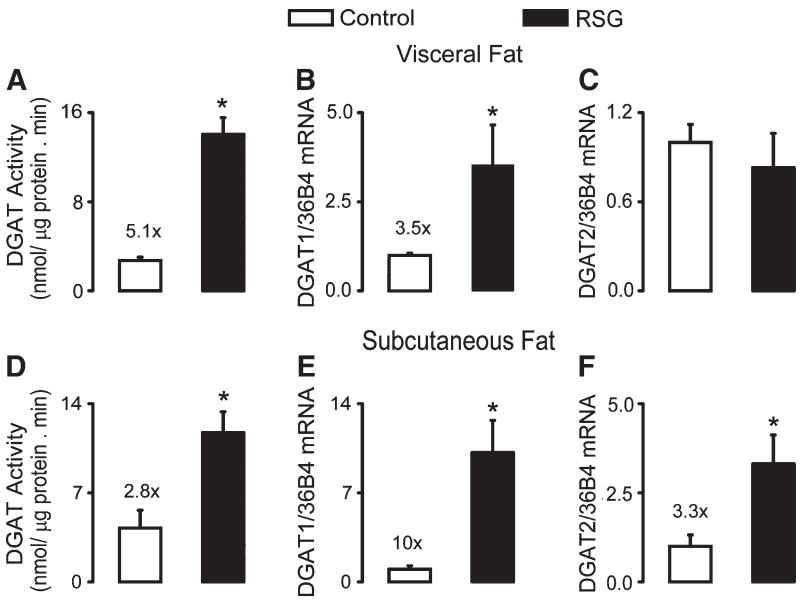

Fig. 7. DGAT activity and mRNA levels of the DGAT isoforms 1 and 2 in VF (A–C) and SF (D–F) of rats treated or not with rosiglitazone (RSG) for 7 days. Each column represents the mean ± SEM of six rats. * $P < 0.05$ versus untreated control.

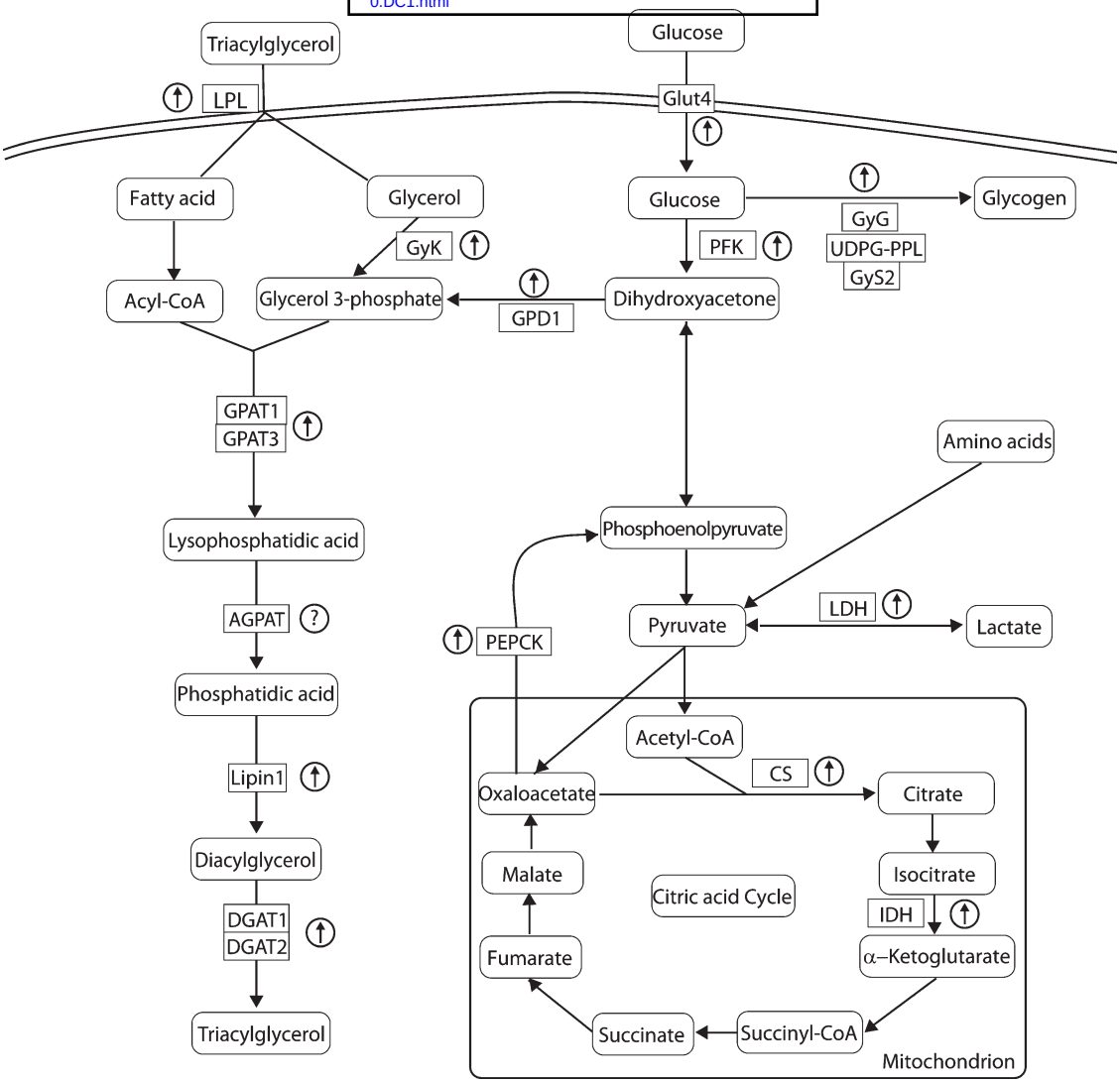

Fig. 8. Schematic representation of the enzymes in the pathways of glucose metabolism and triacylglycerol synthesis affected by rosiglitazone in subcutaneous fat of rats. ↑, upregulated. AGPAT, 1-acylglycerol-3-phosphate *O*-acyltransferase.

tude of the response was much weaker than in SF, and it did not result in alterations of the corresponding metabolic processes. Among other possible implications, this as yet unrecognized induction of energy-generating pathways from glucose in SF by rosiglitazone might be important not only to energetically support the high rates of fatty acid esterification into TAG but also to improve the capacity of WAT to dispose of glucose toward glycogen and TAG-glycerol.

Although to a much lesser absolute extent than oxidation, some glucose disposal in SF was also caused by an enhancement in tissue glycogen synthesis induced by rosiglitazone, as evidenced by the elevated SF rates of glucose incorporation into glycogen and mRNA levels of glycogenin, UDPG-PPL, and GyS2. Although the amount of glucose incorporated into glycogen represents only a small fraction of total WAT glucose metabolism, taking into consideration the marked increase in SF mass induced by PPARγ agonism, this might contribute to the improvement in whole-body glucose homeostasis achieved after longer periods of agonist treatment.

Independently of the fatty acid source (taken up from the circulation, synthesized de novo or recycled from lipolysis), fatty acid esterification into TAG strongly depends upon an adequate supply of glycerol 3-phosphate. Among the three possible sources of glycerol 3-phosphate in WAT, glycerokinase and glyceroneogenesis, as confirmed here by the activity of its key enzyme PEPCK, were previously demonstrated to be activated by rosiglitazone (25–27). Here, we extend these findings by showing that rosiglitazone activates glucose conversion into TAG-glycerol in both VF and SF. In vivo estimation of TAG-glycerol synthesis with $^{3}H_2O$, which allows the estimation of glycerol 3-phosphate synthesis from glucose via both partial glycolysis and glyceroneogenesis, revealed a strong induction by rosiglitazone, an effect that was much more marked in SF than VF, and this confirms in vitro results. PPARγ activation constitutes to date the sole known situation where all three possible sources of glycerol 3-phosphate are concomitantly stimulated in WAT, which further illustrates the importance of PPARγ in the control of fatty acid esterification and TAG synthesis.

In SF, rosiglitazone also markedly enhanced in vitro glucose incorporation into the fatty acid fraction of TAG, an effect that was associated with elevated mRNA levels of G6PDH and ME, proteins involved in the generation of NADPH, and FAS, which catalyzes the last committed steps in the fatty acid synthesis pathway. Such upregulation of fatty acid synthesis from glucose might be the result of rosiglitazone-induced elevation of SREBP1, a well-known regulator of this process (28). Notably, however, increased in vitro fatty acid synthesis from glucose did not translate into an elevation in de novo lipogenesis in vivo as measured with ^3H_2O. This might be because the ^3H_2O technique estimates total fatty acid from all carbon sources to which glucose contributes ~30% in normal nonstimulated conditions (12). Thus, the absence of a change in fatty acid synthesis in vivo in SF might reflect a reduction in the contribution of other carbon sources (lactate, pyruvate, amino acids, acetate, etc.) to this process compensating glucose contribution and keeping total fatty acid synthesis rates unchanged. An alternative explanation for this discrepancy is activation by adiponectin of WAT AMPK (29), which phosphorylates and inhibits acetyl-CoA carboxylase (30), a key enzyme of the de novo fatty acid synthesis pathway. Thus, by increasing adiponectin levels and thereby stimulating the AMPK signaling pathway, rosiglitazone may inhibit the translation of the upregulated lipogenic gene expression and glucose uptake into higher fatty acid synthesis in vivo. Independently of the discrepancies between in vitro and in vivo experiments, and more importantly, the absence of change in de novo fatty acid synthesis in vivo establishes that SF accretion induced by rosiglitazone is associated with an enhanced esterification of preformed, rather than newly synthesized, fatty acids into TAG, which in turn is supported by higher rates of TAG-glycerol synthesis. Of the possible sources of preformed fatty acids, LPL-mediated hydrolysis of lipoprotein-bound TAG appears to be a major supplier of fatty acids to SF, as evidenced here by the elevated tissue LPL activity of rosiglitazone-treated rats compared with controls.

To further elucidate the mechanisms involved in the fat redistribution induced by rosiglitazone, an extensive analysis of the activities and mRNA levels of enzymes involved in TAG synthesis was performed. GPAT, PAP1, and DGAT activities were markedly upregulated by rosiglitazone in both VF and SF, likely the result of increased GPAT1 and 3, lipin 1 and 1B, and DGAT1 expression (mRNA levels), respectively. Of the three enzyme activities investigated, only PAP1 presented a depot-specific effect of rosiglitazone, with SF having a stronger response than VF, an as yet unrecognized effect of PPARγ agonism. Lipin 1 accounts for all the PAP1 activity present in WAT, as revealed in studies with lipin-1-deficient *fld* mice (22). Treatment of human subjects with impaired glucose tolerance with pioglitazone increased the expression of lipin 1B, but not lipin 1A, in subcutaneous adipose tissue. This was accompanied by increased insulin sensitivity (31). The stronger activation of PAP1 activity and lipin 1B expression in SF versus VF may constitute an important component of the fat redistribution process induced by thiazolidinediones. In addition to its role in TAG synthesis, lipin 1 also functions as a transcriptional coactivator for the expression of adipogenic genes (32), raising the possibility of a putative interaction with, and modulation of, PPARγ transcriptional activity by lipin 1. During adipogenesis, PPARγ expression is dependent on the prior activation of the lipin 1A splice variant. The activation of PPARγ (as would occur following rosiglitazone administration) then increases lipin 1B production, which increases the capacity of the adipocytes to accumulate TAG (32). Furthermore, increased expression of lipin 1 in adipose tissue is associated with increased insulin sensitivity despite increased fat accumulation (32). The effects of rosiglitazone in preferentially increasing lipin 1 expression in SF could therefore mediate part of its action as an insulin-sensitizing agent. Further work is needed to explore this hypothesis.

In conclusion, this study showed that the adipose depot specificity of action of PPARγ agonism previously established for lipid metabolism extends to glucose handling. The study identified an SF-specific increase in glucose uptake and its intracellular utilization generating energy and carbon backbones to support the elevated rates of fatty acid esterification into TAG induced by rosiglitazone in this depot. The latter may further be facilitated by the marked upregulation in SF of lipin 1 expression and activity. Taken together, the present findings suggest an involvement of SF glucose metabolism in fat redistribution and improvement in whole-body glucose homeostasis, which are hallmarks of PPARγ agonism.

The authors thank Dr. Z. Yao for providing the lipin-1 antibody. The authors are grateful to Dr. Renato H. Migliorini (in memoriam) for his hospitality and guidance for the lipogenesis work and for the invaluable professional assistance of Maria Antonieta R. Garófalo and Yves Gélinas.

REFERENCES

1. Mori, Y., Y. Murakawa, K. Okada, H. Horikoshi, J. Yokoyama, N. Tajima, and Y. Ikeda. 1999. Effect of troglitazone on body fat distribution in type 2 diabetic patients. *Diabetes Care.* **22:** 908–912.
2. Miyazaki, Y., A. Mahankali, M. Matsuda, S. Mahankali, J. Hardies, K. Cusi, L. J. Mandarino, and R. A. DeFronzo. 2002. Effect of pioglitazone on abdominal fat distribution and insulin sensitivity in type 2 diabetic patients. *J. Clin. Endocrinol. Metab.* **87:** 2784–2791.
3. Smith, S. R., L. De Jonge, J. Volaufova, Y. Li, H. Xie, and G. A. Bray. 2005. Effect of pioglitazone on body composition and energy expenditure: a randomized controlled trial. *Metabolism.* **54:** 24–32.
4. Laplante, M., H. Sell, K. L. MacNaul, D. Richard, J. P. Berger, and Y. Deshaies. 2003. PPAR-gamma activation mediates adipose depot-specific effects on gene expression and lipoprotein lipase activity: mechanisms for modulation of postprandial lipemia and differential adipose accretion. *Diabetes.* **52:** 291–299.
5. DiGirolamo, M., F. D. Newby, and J. Lovejoy. 1992. Lactate production in adipose tissue: a regulated function with extra-adipose implications. *FASEB J.* **6:** 2405–2412.
6. Anghel, S. I., E. Bedu, C. D. Vivier, P. Descombes, B. Desvergne, and W. Wahli. 2007. Adipose tissue integrity as a prerequisite for systemic energy balance: a critical role for peroxisome proliferator-activated receptor gamma. *J. Biol. Chem.* **282:** 29946–29957.
7. Laplante, M., W. T. Festuccia, G. Soucy, Y. Gelinas, J. Lalonde, J. P. Berger, and Y. Deshaies. 2006. Mechanisms of the depot specificity of peroxisome proliferator-activated receptor gamma action on adipose tissue metabolism. *Diabetes.* **55:** 2771–2778.
8. Sokoloff, L., M. Reivich, C. Kennedy, M. H. Des Rosiers, C. S. Patlak, K. D. Pettigrew, O. Sakurada, and M. Shinohara. 1977. The [14C]

deoxyglucose method for the measurement of local cerebral glucose utilization: theory, procedure, and normal values in the conscious and anesthetized albino rat. *J. Neurochem.* **28:** 897–916.
9. Ferre, P., A. Leturque, A. F. Burnol, L. Penicaud, and J. Girard. 1985. A method to quantify glucose utilization in vivo in skeletal muscle and white adipose tissue of the anaesthetized rat. *Biochem. J.* **228:** 103–110.
10. Lo, S., J. C. Russell, and A. W. Taylor. 1970. Determination of glycogen in small tissue samples. *J. Appl. Physiol.* **28:** 234–236.
11. Folch, J., M. Lees, and G. H. Sloane Stanley. 1957. A simple method for the isolation and purification of total lipides from animal tissues. *J. Biol. Chem.* **226:** 497–509.
12. Botion, L. M., M. N. Brito, N. A. Brito, S. R. Brito, I. C. Kettelhut, and R. H. Migliorini. 1998. Glucose contribution to in vivo synthesis of glyceride-glycerol and fatty acids in rats adapted to a high-protein, carbohydrate-free diet. *Metabolism.* **47:** 1217–1221.
13. Jungas, R. L. 1968. Fatty acid synthesis in adipose tissue incubated in tritiated water. *Biochemistry.* **7:** 3708–3717.
14. Windmueller, H. G., and A. E. Spaeth. 1966. Perfusion in situ with tritium oxide to measure hepatic lipogenesis and lipid secretion. Normal and orotic acid-fed rats. *J. Biol. Chem.* **241:** 2891–2899.
15. DiGirolamo, M. 2001. Measurements of glucose conversion to its metabolites. *Methods Mol. Biol.* **155:** 181–192.
16. Chang, H. C., and M. D. Lane. 1966. The enzymatic carboxylation of phosphoenolpyruvate. II. Purification and properties of liver mitochondrial phosphoenolpyruvate carboxykinase. *J. Biol. Chem.* **241:** 2413–2420.
17. Festuccia, W. T., N. H. Kawashita, M. A. Garofalo, M. A. Moura, S. R. Brito, I. C. Kettelhut, and R. H. Migliorini. 2003. Control of glyceroneogenic activity in rat brown adipose tissue. *Am. J. Physiol. Regul. Integr. Comp. Physiol.* **285:** R177–R182.
18. Smith, P. K., R. I. Krohn, G. T. Hermanson, A. K. Mallia, F. H. Gartner, M. D. Provenzano, E. K. Fujimoto, N. M. Goeke, B. J. Olson, and D. C. Klenk. 1985. Measurement of protein using bicinchoninic acid. *Anal. Biochem.* **150:** 76–85.
19. Lewin, T. M., S. Wang, C. A. Nagle, C. G. Van Horn, and R. A. Coleman. 2005. Mitochondrial glycerol-3-phosphate acyltransferase-1 directs the metabolic fate of exogenous fatty acids in hepatocytes. *Am. J. Physiol. Endocrinol. Metab.* **288:** E835–E844.
20. Schlossman, D. M., and R. M. Bell. 1976. Triacylglycerol synthesis in isolated fat cells. Evidence that the sn-glycerol-3-phosphate and dihydroxyacetone phosphate acyltransferase activities are dual catalytic functions of a single microsomal enzyme. *J. Biol. Chem.* **251:** 5738–5744.
21. Coleman, R., and R. M. Bell. 1976. Triacylglycerol synthesis in isolated fat cells. Studies on the microsomal diacylglycerol acyltransferase activity using ethanol-dispersed diacylglycerols. *J. Biol. Chem.* **251:** 4537–4543.
22. Donkor, J., M. Sariahmetoglu, J. Dewald, D. N. Brindley, and K. Reue. 2007. Three mammalian lipins act as phosphatidate phosphatases with distinct tissue expression patterns. *J. Biol. Chem.* **282:** 3450–3457.
23. Manmontri, B., M. Sariahmetoglu, J. Donkor, M. B. Khalil, M. Sundaram, Z. Yao, K. Reue, R. Lehner, and D. N. Brindley. 2008. Glucocorticoids and cyclic AMP selectively increase hepatic lipin-1 expression, and insulin acts antagonistically. *J. Lipid Res.* **49:** 1056–1067.
24. Festuccia, W. T., S. Oztezcan, M. Laplante, M. Berthiaume, C. Michel, S. Dohgu, R. G. Denis, M. N. Brito, N. A. Brito, D. S. Miller, et al. 2008. Peroxisome proliferator-activated receptor-γ-mediated positive energy balance in the rat is associated with reduced sympathetic drive to adipose tissues and thyroid status. *Endocrinology.* **149:** 2121–2130.
25. Guan, H. P., Y. Li, M. V. Jensen, C. B. Newgard, C. M. Steppan, and M. A. Lazar. 2002. A futile metabolic cycle activated in adipocytes by antidiabetic agents. *Nat. Med.* **8:** 1122–1128.
26. Tontonoz, P., E. Hu, J. Devine, E. G. Beale, and B. M. Spiegelman. 1995. PPAR gamma 2 regulates adipose expression of the phosphoenolpyruvate carboxykinase gene. *Mol. Cell. Biol.* **15:** 351–357.
27. Festuccia, W. T., M. Laplante, M. Berthiaume, Y. Gelinas, and Y. Deshaies. 2006. PPARgamma agonism increases rat adipose tissue lipolysis, expression of glyceride lipases, and the response of lipolysis to hormonal control. *Diabetologia.* **49:** 2427–2436.
28. Wang, S. L., E. Z. Du, T. D. Martin, and R. A. Davis. 1997. Coordinate regulation of lipogenesis, the assembly and secretion of apolipoprotein B-containing lipoproteins by sterol response element binding protein 1. *J. Biol. Chem.* **272:** 19351–19358.
29. Wu, X., H. Motoshima, K. Mahadev, T. J. Stalker, R. Scalia, and B. J. Goldstein. 2003. Involvement of AMP-activated protein kinase in glucose uptake stimulated by the globular domain of adiponectin in primary rat adipocytes. *Diabetes.* **52:** 1355–1363.
30. Hardie, D. G., and D. A. Pan. 2002. Regulation of fatty acid synthesis and oxidation by the AMP-activated protein kinase. *Biochem. Soc. Trans.* **30:** 1064–1070.
31. Yao-Borengasser, A., N. Rasouli, V. Varma, L. M. Miles, B. Phanavanh, T. N. Starks, J. Phan, H. J. Spencer 3rd, R. E. McGehee, Jr., K. Reue, et al. 2006. Lipin expression is attenuated in adipose tissue of insulin-resistant human subjects and increases with peroxisome proliferator-activated receptor gamma activation. *Diabetes.* **55:** 2811–2818.
32. Reue, K., and D. N. Brindley. 2008. Thematic Review Series: Glycerolipids. Multiple roles for lipins/phosphatidate phosphatase enzymes in lipid metabolism. *J. Lipid Res.* **49:** 2493–2503.